

ChemComm

Accepted Manuscript



This is an *Accepted Manuscript*, which has been through the Royal Society of Chemistry peer review process and has been accepted for publication.

Accepted Manuscripts are published online shortly after acceptance, before technical editing, formatting and proof reading. Using this free service, authors can make their results available to the community, in citable form, before we publish the edited article. We will replace this *Accepted Manuscript* with the edited and formatted *Advance Article* as soon as it is available.

You can find more information about *Accepted Manuscripts* in the [Information for Authors](#).

Please note that technical editing may introduce minor changes to the text and/or graphics, which may alter content. The journal's standard [Terms & Conditions](#) and the [Ethical guidelines](#) still apply. In no event shall the Royal Society of Chemistry be held responsible for any errors or omissions in this *Accepted Manuscript* or any consequences arising from the use of any information it contains.

COMMUNICATION

Facile synthesis of spinel CuCo_2O_4 nanocrystal as a high-performance cathode catalyst for rechargeable Li-air batteries †

Cite this: DOI: 10.1039/x0xx00000x

Received 00th January 2012,
Accepted 00th January 2012

DOI: 10.1039/x0xx00000x

www.rsc.org/

Ying Liu^a, Lu-Jie Cao^b, Chen-Wei Cao^a, Man Wang^a, Kwan-Lan Leung^a, Shan-Shan Zeng^a, T. F. Hung^a, C. Y. Chung^{a*}, Zhou-Guang Lu^{b*}

CuCo_2O_4 nanoparticles have been synthesized by a simple and low-cost urea combustion method and characterized as a bifunctional catalyst for non-aqueous Li-air batteries. The resulting CuCo_2O_4 catalyst has been demonstrated to effectively reduce the charge/discharge polarization of Li-air batteries in a simulated air environment (80% Ar: 20% O_2).

Rechargeable non-aqueous lithium-air batteries have been the focus of current research interest due to their significantly high gravimetric energy (3505 Wh kg^{-1} based on the reversible reaction of $2\text{Li} + \text{O}_2 \rightarrow \text{Li}_2\text{O}_2$).¹⁻⁴ It can deliver 5-10 times higher gravimetric energy density than lithium ion batteries because oxygen, the cathode active material, is not stored in the battery, that can be accessible from the ambient environment.^{5,6} Thus, Li-air batteries have been considered as promising candidates for electric-vehicle applications. However, in practice, the development of Li-air batteries faces several challenges, such as electrolyte instability, low round-trip efficiency, low power capability, and poor cycle life.⁷⁻⁹

A typical rechargeable non-aqueous Li-air battery is comprised of a Li metal electrode, Li conducting organic electrolyte and a porous O_2 -breathing catalytic electrode. The reversible formation/decomposition of Li_2O_2 on discharge and charge occurs at three-phase boundary that contains solid electrode, liquid electrolyte and oxygen gas, leading to sluggish kinetics of oxygen reduction reaction (ORR) and oxygen evolution reaction (OER).¹⁰⁻¹³ Furthermore, weak interaction between O_2 and the electrode not only limits the supply of O_2 to reaction, but also the electrolyte and O_2 diffusion pathways are hampered by the insoluble solid discharge product (Li_2O_2) into the pores. It is reported that the kinetic reactions can be considerably accelerated by employing sophisticated cathode and effective electrocatalysts.¹⁴⁻¹⁶ Thus, a variety of electrocatalysts including carbon,^{5, 17-19} noble metals,^{3, 20, 21} transition metal oxides²²⁻²⁵ and metal nitrides²⁶⁻²⁸ have been used as the cathode catalysts in the Li-oxygen batteries to

reduce the charge/discharge overpotential to enhance the energy efficiency.

Co_3O_4 with the advantages of high activity and stability has been identified to be a catalytically active material for a non-aqueous Li-air battery.^{11, 29, 30} However, because cobalt is toxic and high cost, it is significant to replace Co with low-cost and eco-friendly element to obtain a spinel structure compound. For example, MnCo_2O_4 and CoFe_2O_4 have been reported as effective catalysts for Li-air batteries,^{31, 32} while CuCo_2O_4 has been utilized as the active material for supercapacitors and Li ion batteries.^{33, 34} Spinel CuCo_2O_4 supported on the N-doped reduced graphene oxide exhibits higher ORR catalytic activity and superior durability as compared to the commercial Pt/C catalyst.³⁵ More importantly, copper-based materials have exhibited excellent ORR and OER catalytic activity due to the strong interface contact of Cu and its surrounding.³⁶ However, to the best of our knowledge, no literatures have reported about the application of CuCo_2O_4 nanoparticles for Li-air batteries. In this work, a simple urea combustion method combined with a post annealing process was used to prepare CuCo_2O_4 nanoparticles and its electrocatalytic activity as a catalyst for Li-air batteries was investigated in detail.

CuCo_2O_4 nanoparticles were synthesized using nitrate salts as precursors and urea as fuel at low temperature (see Experimental section for details, ESI†). CuCo_2O_4 adopts the cubic spinel structure with the space group $\text{Fd}3\text{m}$ and all of the diffraction peaks in this pattern match very well with the JCPDS file no. 78-2177 (Fig. 1a). The simulated structural model provides clear information about the crystal structure of the spinel CuCo_2O_4 ; in which Cu and Co randomly occupy the tetrahedral sites and octahedral sites (Fig. 1b).

Typical scanning electron microscopy (SEM) (Fig. S1, ESI†) and transmission electron microscopy (TEM) (Fig. 2a and b) images show that the as-synthesized sample is composed of irregular sphere microstructures with segregated particles. The size distribution of fine nanoparticles is ranging from 2-18 nm with a calculated average of 8 nm (Fig. S2, ESI†). In the HRTEM image

(Fig. 2c), the measured distance between adjacent lattice fringes is about 0.24 nm, in accordance with the (311) plane of CuCo_2O_4 . The corresponding SAED pattern shown in Fig. 2d demonstrates the poly-crystalline nature of the as-obtained CuCo_2O_4 . The characteristic diffraction spots can be assigned to the facets of (220), (311), (222) and (422) of CuCo_2O_4 .

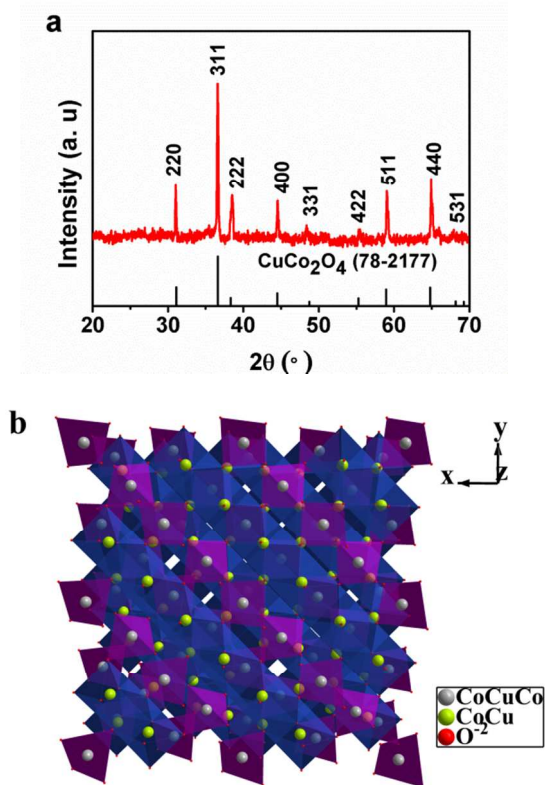


Fig. 1 (a) XRD pattern of the synthesized CuCo_2O_4 nanoparticles and (b) structure model of the CuCo_2O_4 phase.

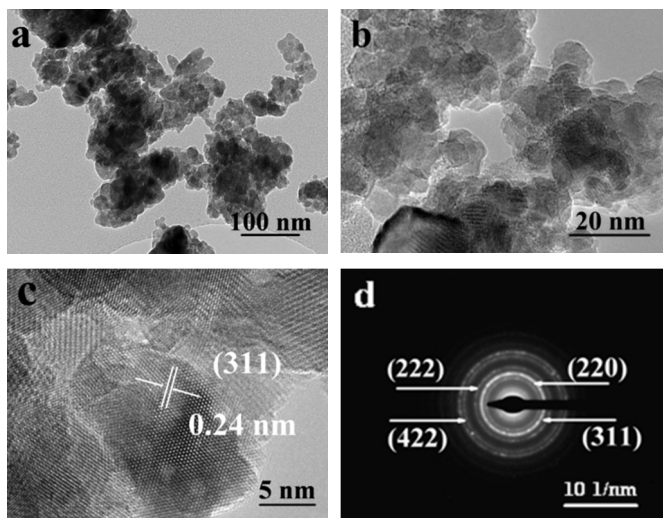


Fig. 2 (a and b) TEM images and (c) HRTEM image of the synthesized CuCo_2O_4 nanoparticles. (d) The SAED pattern showing diffuse rings indicating CuCo_2O_4 phase. The assigned Miller indices (hkl) to the marked rings are shown.

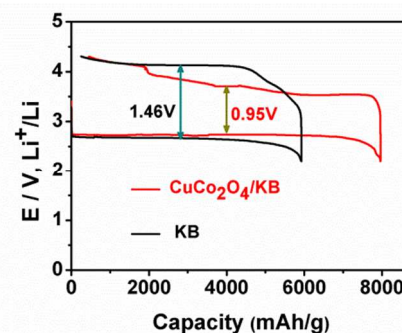


Fig. 3 The 1st cycle discharge/charge profiles of the Li-air batteries with $\text{CuCo}_2\text{O}_4/\text{KB}$ composite and KB as catalyst at a current density of 50 mA g^{-1} .

The O_2 cathode was prepared by coating a paste of the CuCo_2O_4 sample (30 wt%), KB (60 wt%) and polytetrafluoroethylene (10 wt%) onto carbon paper disks. In order to prevent Li foil from reacting with water and gases other than oxygen gas from the air, the cells were tested by using TEGEME-based electrolyte under $\text{Ar}:\text{O}_2$ (80%: 20%) atmosphere. The first discharge and charge curves of the Li-air batteries with CuCo_2O_4 are compared with those of the Li-air batteries with the pristine KB at a current density of 50 mA g^{-1} with a cutoff voltage of 2.2 V as shown in Fig. 3. The Li-air battery with CuCo_2O_4 presents a discharge-recharge polarization of 0.95 V (0.51 V smaller than those of the KB-only cathode). Sudden decay of the battery with $\text{CuCo}_2\text{O}_4/\text{KB}$ around 4 V is observed because of the oxidation of electrolyte.^{11, 22} CV curves present that $\text{CuCo}_2\text{O}_4/\text{KB}$ electrode exhibits a lower anodic peak voltage and higher larger ORR/OER peak current as compared with KB only electrode (Fig. S3, ESI[†]). Furthermore, the battery with $\text{CuCo}_2\text{O}_4/\text{KB}$ or KB delivers high capacities of 7962 mAh g^{-1} , which is much higher than that of the one with only KB (about 5920 mAh g^{-1}) and blank carbon paper (about 298 mAh g^{-1}) (Fig. S4, ESI[†]).

The effects of current on the discharge/charge voltages of Li-air batteries with $\text{CuCo}_2\text{O}_4/\text{KB}$ electrode have been further investigated. With a cut-off capacity of 1000 mAh g^{-1} and at current density ranging from 100 to 400 mA g^{-1} , Li-air batteries are discharged and charged for 50 cycles and the corresponding profiles are depicted in Fig. 4. Beyond the initial 20 cycles, the discharge potential is gradually decreased and reaches below 2.5 V at the end of the 50th cycle, as shown in Fig. 4a. The coulombic efficiency after continuous 50 cycles remains to be higher than 86.5% at a current density of 100 mA g^{-1} . This is closely related to the superior ORR and OER catalytic activities of CuCo_2O_4 nanoparticles. The introduction of Cu^{2+} into Co_3O_4 lattice can enhance the cycling performance of battery at higher current density (Fig. S5, ESI[†]). When the current density is increased to 400 mA g^{-1} , the cells survive for more than 20 cycles, as shown in Fig. 4c and 4d. The discharge potential in a simulated air environment is decreased obviously and reaches the lower potential limit of 2.0 V, while the charge potential is increased quickly and reaches the upper potential limit of 4.7 V. Besides, the discharge capacity is higher than the corresponding charge capacity after 28 cycles with the charge potential higher than 4.14 V in Fig. 4c at 400 mA g^{-1} . It is indicated that there may exist a significant increase in the polarization of Li foil, which is mainly ascribed to the rise in the electrode resistance.^{2, 3} The increase in the cell resistance is attributed to the accumulation of discharge products due to the incomplete decomposition during charge (Fig. S6, ESI[†]).³⁷ However, comparing with pure KB carbon, the CuCo_2O_4 air electrode has better rechargeability

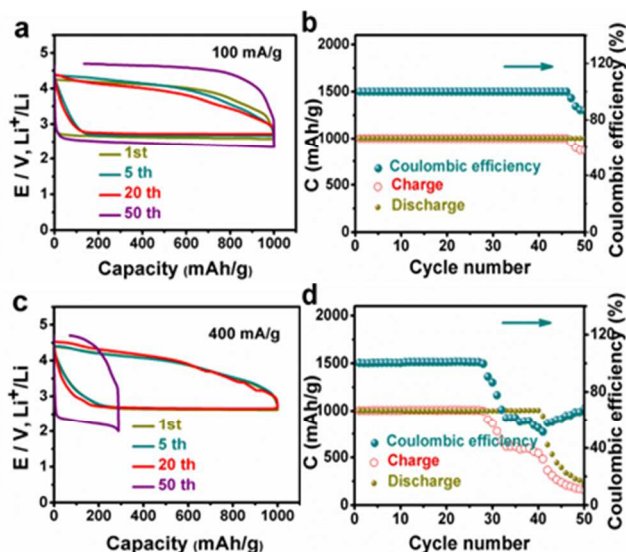


Fig. 4 Discharge/charge profiles of the Li-air batteries with $\text{CuCo}_2\text{O}_4/\text{KB}$ cathode over 50 cycles with a cut-off capacity of 1000 mAh g^{-1} , at a current density of 100 mA g^{-1} (a), 400 mA g^{-1} (c) and the corresponding cyclability and coulombic efficiency (b) and (d).

performance at 400 mA g^{-1} while the pure KB electrode can merely sustain less than 12 cycles (Fig. S7, ESI†). In the simulated air condition, the electrochemical performance of CuCo_2O_4 electrode may be compared to the reported catalysts tested in pure O_2 (Tab. S1, ESI†).

To identify the discharge/charge products of Li-air batteries with $\text{CuCo}_2\text{O}_4/\text{KB}$ cathode, XRD patterns of the $\text{CuCo}_2\text{O}_4/\text{KB}$ cathode after the first discharge and charge processed at a current of 100 mA g^{-1} were collected, as shown in Fig. 5. As compared with XRD pattern of the pristine electrode, some additional diffraction centered at 23.05° , 32.77° , 34.83° and 58.50° are observed for the discharged electrode, which can be indexed to the (002), (200), (201) and (220) peaks of Li_2O_2 , respectively, indicating that Li_2O_2 is formed during discharge and is the major crystalline discharge product (Fig. S8, ESI†). When the Li-air battery is recharged to 4.25 V, the diffraction peaks of Li_2O_2 disappear since the formed Li_2O_2 is decomposed. This further suggests that the discharging and charging processes of Li-air batteries are actually the reversible formation and decomposition of Li_2O_2 , which is well agree with many reported references.^{7, 19, 38} SEM was conducted to investigate the deactivation mechanism of $\text{CuCo}_2\text{O}_4/\text{KB}$ cathode after 28 cycles (Fig. S9, ESI†). Before discharge, it is obvious that CuCo_2O_4 and KB particles are deposited on the surface of initial electrode. After 3 cycles, the absence of the toroidal Li_2O_2 can be observed on the surface of the $\text{CuCo}_2\text{O}_4/\text{KB}$ electrode. After 28 cycles, the surface of electrode is covered by the discharge products with poor electronic conductivity, and it blocks the pathways for oxygen diffusion and electron transfer, then leading to the performance deterioration of Li-air batteries.^{11, 20} However, for the KB electrode, after 3 cycles, massive blocks still remain after complete charge, revealing that only part of Li_2O_2 is decomposed in the charging process. The results here clearly demonstrate that CuCo_2O_4 have significant influence on catalysing the oxidation of Li_2O_2 during the recharging process. Furthermore, it is concluded that the CuCo_2O_4 nanoparticles favor the reversible formation and decomposition of Li_2O_2 and thus enhance charge-discharge efficiency and cyclability of the

assembled Li-air batteries. The high catalytic performance of CuCo_2O_4 is ascribed to the strong

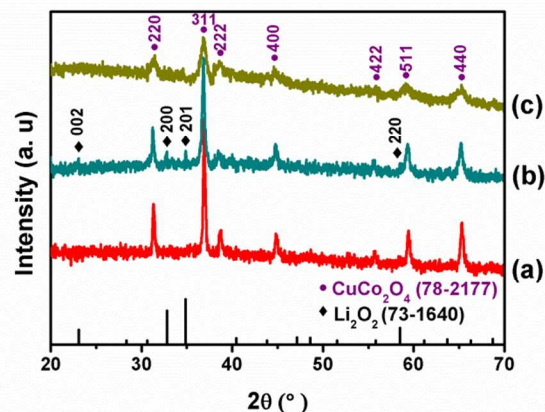


Fig. 5 XRD patterns of the pristine (a), the 1st-cycle discharged (b), and charged (c) $\text{CuCo}_2\text{O}_4/\text{KB}$ cathode. The samples were collected after being scratched from the carbon paper.

interface interactions between Cu and Co_3O_4 , thus resulting in the increase of active sites on Cu-based catalyst.^{36, 39} Besides, the defect structure of CuCo_2O_4 from the ionic radius difference of Cu^{2+} and Co^{3+} ions can provide favourable catalytic active centres for Li-air batteries.

In summary, spinel CuCo_2O_4 nanoparticles prepared via a facile urea combustion method can be promising bifunctional electrocatalyst for Li-air batteries. Compared with the traditional KB carbon electrode, the $\text{CuCo}_2\text{O}_4/\text{KB}$ electrode exhibits much lower polarization, better rate capability and longer cycling life. In a stimulated air condition, the cell delivers a high capacity of 7962 mAh g^{-1} with a discharge-recharge voltage gap of 0.95 V at 50 mA g^{-1} . With a cut-off capacity of 1000 mAh g^{-1} at 400 mA g^{-1} , the Li-air battery with $\text{CuCo}_2\text{O}_4/\text{KB}$ can be discharged and charged for 28 cycles. This indicates the superior ORR and OER catalytic activity of CuCo_2O_4 . Furthermore this method is simple, low-cost, easy for scale up and controllable.

This work is financially supported by Hong Kong SAR government Research Grant Council. LZG would like to acknowledge the support from the Starting-Up Funds of South University of Science and Technology of China (SUSTC).

Notes and references

- ^a Department of Physics and Materials Science, City University of Hong Kong, Hong Kong SAR, PR China. E-mail: appchung@cityu.edu.hk
^b Department of Materials Science & Engineering, South University of Science and Technology of China, Shenzhen, PR China. E-mail: luzg@sustc.edu.cn

† Electronic Supplementary Information (ESI) available: Experimental details and Fig. S1-S9. See DOI: 10.1039/c000000x/

- H. G. Jung, J. Hassoun, J. B. Park, Y. K. Sun, and B. Scrosati, *Nat. chem.*, 2012, **4**, 579.
- F. J. Li, T. Zhang, Y. K. Yamada, A. Yamada, and H. S. Zhou, *Adv. Energy Mater.*, 2013, **3**, 532.
- Z. L. Jian, P. Liu, F. J. Li, P. He, X. W. Guo, M. W. Chen, and H. S. Zhou, *Angew. Chem. Int. Ed.*, 2014, **53**, 442.
- P. G. Bruce, S. A. Freunberger, L. J. Hardwick, and J. M. Tarascon, *Nat.*

- mater.*, 2012, **11**, 19.
- 5 R. R. Mitchell, B. M. Gallant, C. V. Thompson, and Y. Shao-Horn, *Energy Environ. Sci.*, 2011, **4**, 2952.
- 6 D. A. Tompsett and M. S. Islam, *Chem. Mater.*, 2013, **25**, 2515.
- 7 Z. Peng, S. A. Freunberger, Y. Chen, and P. G. Bruce, *Science*, 2012, **337**, 563.
- 8 Y. Y. Shao, F. Ding, J. Xiao, J. Zhang, W. Xu, S. Park, J. G. Zhang, Y. Wang, and J. Liu, *Adv. Funct. Mater.*, 2013, **23**, 987.
- 9 J. J. Xu, D. Xu, Z. L. Wang, H. G. Wang, L. L. Zhang, and X. B. Zhang, *Angew. Chem. Int. Ed.*, 2013, **52**, 3887.
- 10 G. Girishkumar, B. McCloskey, A. C. Luntz, S. Swanson, and W. Wilcke, *J. Phys. Chem. Lett.*, 2010, **1**, 2193.
- 11 R. Black, J. H. Lee, B. Adams, C. A. Mims, and L. F. Nazar, *Angew. Chem.*, 2013, **125**, 410.
- 12 B. D. McCloskey, D. S. Bethune, R. M. Shelby, G. Girishkumar, and A. Luntz, *J. Phys. Chem. Lett.*, 2011, **2**, 1161.
- 13 B. D. McCloskey, R. Scheffler, A. Speidel, D. S. Bethune, R. M. Shelby, and A. Luntz, *J. Am. Chem. Soc.*, 2011, **133**, 18038.
- 14 K. Guo, Y. Li, J. Yang, Z. Q. Zou, X. Z. Xue, X. M. Li, and H. Yang, *J. Mater. Chem. A*, 2014, **2**, 1509.
- 15 T. Zhang and H. S. Zhou, *Nature commun.*, 2013, **4**, 1817.
- 16 H. D. Lim, H. Song, J. Kim, H. Gwon, Y. Bae, K. Y. Park, J. Hong, H. Kim, T. Kim, and Y. H. Kim, *Angew. Chem. Int. Ed.*, 2014, **53**, 3926.
- 17 Z. Y. Guo, D. D. Zhou, X. L. Dong, Z. J. Qiu, Y. G. Wang, and Y. Y. Xia, *Adv. Mater.*, 2013, **25**, 5668.
- 18 J. L. Shui, F. Du, C. M. Xue, Q. Li, and L. M. Dai, *ACS nano*, 2014, **8**, 3015.
- 19 H. R. Byon, B. M. Gallant, S. W. Lee, and Y. Shao-Horn, *Adv. Funct. Mater.*, 2013, **23**, 1037.
- 20 F. J. Li, D. M. Tang, Y. Chen, D. Golberg, H. Kitaura, T. Zhang, A. Yamada, and H. S. Zhou, *Nano lett.*, 2013, **13**, 4702.
- 21 G. Y. Zhao, J. X. Lv, Z. M. Xu, L. Zhang, and K. N. Sun, *J. Power Sources*, 2014, **248**, 1270.
- 22 Z. H. Cui, X. X. Guo, *J. Power Sources*, 2014, **267**, 20.
- 23 Z. Zhang, L. W. Su, M. Yang, M. Hu, J. Bao, J. P. Wei and Z. Zhou, *Chem. Commun.*, 2013, **50**, 776.
- 24 X. F. Hu, X. P. Han, Y. X. Hu, F. Y. Cheng, and J. Chen, *Nanoscale*, 2014, **6**, 3522.
- 25 Y. Cao, Z. K. Wei, J. He, J. Zang, Q. Zhang, M. S. Zheng, and Q. F. Dong, *Energy Environ. Sci.*, 2012, **5**, 9765.
- 26 J. Park, Y. S. Jun, W. R. Lee, J. A. Gerbec, K. A. See, and G. D. Stucky, *Chem. Mater.*, 2013, **25**, 3779.
- 27 F. J. Li, R. Ohnishi, Y. Yamada, J. Kubota, K. Domen, A. Yamada, and H. S. Zhou, *Chem. Commun.*, 2013, **49**, 1175.
- 28 K. J. Zhang, L. X. Zhang, X. Chen, X. He, X. G. Wang, S. M. Dong, P. X. Han, C. J. Zhang, S. Wang, L. Gu, and G. L. Cui, *J. Phys. Chem. C*, 2013, **117**, 858.
- 29 W. H. Ryu, T. H. Yoon, S. H. Song, S. Jeon, Y. J. Park, and I. D. Kim, *Nano Lett.* 2013, **13**, 4190.
- 30 C. W. Sun, F. Li, C. Ma, Y. Wang, Y. L. Ren, W. Yang, Z. H. Ma, J. J. Li, Y. J. Chen, Y. Kim, and L. Q. Chen, *J. Mater. Chem. A*, 2014, **2**, 7188.
- 31 H. L. Wang, Y. Yang, Y. Y. Liang, G. Y. Zheng, Y. G. Li, Y. Cui, and H. J. Dai, *Energy Environ. Sci.*, 2012, **5**, 7931.
- 32 Q. F. Dong, Y. Cao, S. R. Cai, S. C. Fan, W. Hu, and M. S. Zheng, *Faraday Discuss.*, 2014, DOI: 10.1039/C4FD00075G.
- 33 A. Pendashteh, M. S. Rahmanifar, R. B. Kaner, and M. F. Mousavi, *Chem. Commun.*, 2014, **50**, 1972.
- 34 Q. F. Wang, J. Xu, X. F. Wang, B. Liu, X. J. Hou, G. Yu, P. Wang, D. Chen, and G. Z. Shen, *ChemElectroChem.*, 2013, **1**, 559.
- 35 R. Ning, J. Q. Tian, A. M. Asiri, A. H. Qusti, A. O. AlYoubi, and X. P. Sun, *Langmuir*, 2013, **29**, 13146.
- 36 M. Jahan, Z. L. Liu, and K. P. Loh, *Adv. Funct. Mater.*, 2013, **23**, 5363.
- 37 X. P. Han, Y. X. Hu, J. G. Yang, F. Y. Cheng, and J. Chen, *Chem. Commun.*, 2014, **50**, 1497.
- 38 Z. K. Luo, C. S. Liang, F. Wang, Y. H. Xu, J. Chen, D. Liu, H. Y. Sun, H. Yang, and X. P. Fan, *Adv. Funct. Mater.*, 2013, **24**, 2101.
- 39 A. Débart, J. L. Bao, G. Armstrong, P. G. Bruce, *J. Power Sources*, 2007, **174**, 1177.

COMMUNICATION

Facile synthesis of spinel CuCo_2O_4 nanocrystal as a high-performance cathode catalyst for rechargeable Li-air batteries †

Ying Liu^a, Lu-Jie Cao^b, Chen-Wei Cao^a, Man Wang^a, Kwan-Lan Leung^a, Shan-Shan Zeng^a, T. F. Hung^a, C. Y. Chung^{a*}, Zhou-Guang Lu^{b*}

Abstract

CuCo_2O_4 nanoparticles have been synthesized by a simple and low-cost urea combustion method and characterized as a bifunctional catalyst for non-aqueous Li-air batteries. The resulting CuCo_2O_4 catalyst has been demonstrated to effectively reduce the charge/discharge polarization of Li-air batteries in a simulated air environment (80% Ar: 20% O_2).

